J. Plasma Fusion Res. SERIES, Vol. 4 (2001) 383–386

On the Ion Distribution Function around the Plug in a Tandem Mirror

KATANUMA Isao*, ITO Toru, SHIOTANI Kensuke, TATEMATSU Yoshinori, ISHII Kameo, SAITO Teruo and YATSU Kiyoshi

Plasma Research Center, University of Tsukuba, Tsukuba 305-8577, Japan

(Received: 5 December 2000 / Accepted: 27 August 2001)

Abstract

It is shown that the plug potential is formed only with flow ions accelerated by the thermal barrier potential and non-Maxwellian electrons due to the electron cyclotron resonance heating in the plug/thermal barrier region of a tandem mirror. For the purpose to display the plug potential formation, the Monte-Carlo simulation has been carried out, where the effect of coulomb collisions are included.

Keywords:

plug potential, tandem mirror, thermal barrier, orbit, Monte-Carlo simulation

1. Introduction

We have shown that the plug potential is formed with only electron cyclotron resonance heating (ECRH) around the plug region in the tandem mirror [1-4]. The essential mechanism for the plug potential formation is believed to be made clear in these works. However, the several assumptions have been made for the calculation of the plug potential formation. One is that the ion and electron distribution functions are given a priori at the thermal barrier region. The small angle scattering of ions during its flight from outer mirror throat to the potential maximum is assumed in the given distribution function.

The ion distribution has not been measured in the plug/thermal region yet, so that the comparison of the assumption with the experiments has not been made. Therefore, the purpose of this paper is that the plug potential is shown to be formed under more realistic condition.

2. Numerical Method

In this section we briefly show the Monte-Carlo simulation code, where the detailed information will be found in refs. [5-7]. Although this code adopts the flux coordinates in the tandem mirror, only one-dimensional motion along axis is followed in this paper. The effects of coulomb collision are included with help of Monte-Carlo method [5].

Figure 1 shows the plug/barrier mirror cell of the GAMMA10 tandem mirror, where a half mirror cell is considered. Ions are input at the inner mirror throat of the plug/barrier mirror cell, where the magnitude of magnetic field at the inner mirror throat is the same as that at the outer mirror throat $z = z_m$ in GAMMA10. The ions input at the inner mirror throat have the velocity with a random number giving Maxwellian distribution of temperature T_i, and the input ions are accelerated by the thermal barrier potential at the thermal barrier $z = z_b$. Therefore, the distribution function of the input ions at $z = 0$ is Maxwellian in the region $\varepsilon - \mu B_i - e\varphi_i \geq 0$ and $\varepsilon - \mu B_b - e\varphi_b \geq 0$, and no ions in the other regions in the velocity space. Here we use the standard notations through this paper and ε is energy of ion and μ is the magnetic moment. The subscripts i and b represent the quantities at the inner mirror throat and thermal barrier,

*Corresponding author's e-mail: katanuma@prc.tsukuba.ac.jp

respectively.

The ions, which reflect at the midway in the mirror cell by the magnetic field and electrostatic potential and then come back again at $z = 0$, are assumed to be lost, that is, the ions trapped in the thermal barrier cell are lost within one transit time. The ions passing through the outer mirror throat $z = z_m$ are assumed to be lost to the end-wall. The ions moving in the mirror cell receive a coulomb collision with the field particles (consist of ions and electrons with density 10^{11} cm^{-3}, temperature 100eV). Those procedures are repeated until a steady state is realized.

The equation of motion is given as

$$\frac{dz}{dt} = v_{\parallel},$$
$$v_{\parallel} = \sqrt{\frac{2}{m_i}(\varepsilon - \mu B(z) - e\varphi(z))}, \qquad (1)$$

where z is the axial coordinate.

The electron's motion is not included in this calculation. Instead the electron distribution function is given in advance and the axial potential profile is determined from the ion density and electron distribution function i.e., modified Boltzmann law is used. In this paper we assume the electron distribution function as

$$f_e = n_b \left(\frac{m_e}{2\pi}\right)^{3/2} \frac{1}{T_{e\parallel}^{1/2} T_{e\perp}} \exp\left\{-\frac{\varepsilon + e\varphi_b}{T_{e\parallel}} - \left(\frac{1}{T_{e\perp}} - \frac{1}{T_{e\parallel}}\right)\mu B_b\right\}, \qquad (2)$$

which gives the modified Boltzmann law i.e.,

$$\varphi(z) = \frac{T_{e\parallel}}{e} \ln\left\{\left[\frac{T_{e\perp}}{T_{e\parallel}} + \left(1 - \frac{T_{e\perp}}{T_{e\parallel}}\right)\frac{B_b}{B(z)}\right]\frac{n(z)}{n_b}\right\}. \qquad (3)$$

It is known that the ion acoustic waves appear when eqs. (1) and (3) are taken into account. However we are interested in the steady state of the system, so that the waves are removed by time averaging which is shown in the following.

The initial condition is shown in Fig. 1, where ions are distributed at regular intervals along z-axis. The electrostatic potential $e\varphi(z)/T_i = -2.0$ at first. The calculation is started at this initial state. On the other hand, the electrostatic potential is not changed in time but only ions' motion is calculated until the steady state of ion density axial profile is realized. The electrostatic potential is calculated by eq. (3) and the steady state ion density profile assuming charge neutrality condition,

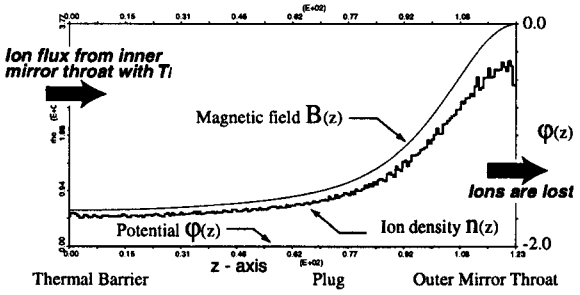

Fig. 1 Axial profile of magnetic field of GAMMA10, where a half of the plug/barrier mirror cell is shown. The initial state of ion density profile determined by their axial positions and initial electrostatic potential are also shown.

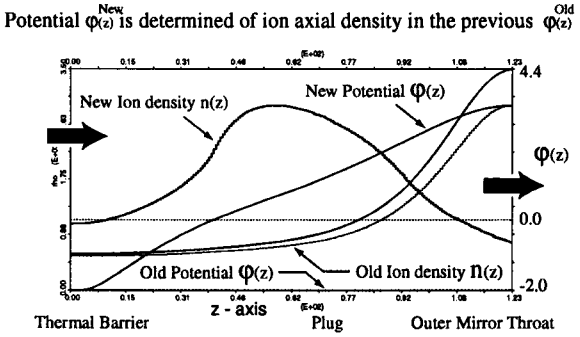

Fig. 2 The situation how to determine the steady state electrostatic potential axial profile.

where is shown in Fig. 2.

In Fig. 2 the ion densities "Old Ion density" and "New Ion density" are in the steady state obtained by the Monte-Carlo simulation in the electrostatic potential "Old Potential" and "New Potential", respectively. That is, the Monte-Carlo simulation is carried out until its steady state of ion density profile is come, in the given electrostatic potential profile. The electrostatic potential in the next step is determined by eq. (3) and the steady state ion density profile as the "New potential $\varphi(z)$". The calculation is carried out in this New electrostatic potential until the new steady state of ion density profile is realized again. The above procedure is repeated until the steady state of the electrostatic potential is realized.

3. Numerical Results

As seen in ref. [1,3] the plug potential formation should satisfy the condition that

$$n_i(\varphi_p, B_p) = n_e(\varphi_p, B_p),$$
$$\frac{\partial n_i}{\partial B_p} = \frac{\partial n_e}{\partial B_p}, \quad (4)$$

at the plug.

As long as the electron distribution function is Maxwellian i.e., $T_{e\parallel} = T_{e\perp}$ in eq. (3), the relation $\partial n_e/\partial B_p = 0$ is hold. Therefore, the peak position of the density profile coincided with the maximum point of the potential profile, which indicates that the large plug potentialis not formed.

The ions are reflected in front of the plug potential, (note bulk ion energy with thermal velocity is much smaller than the plug potential) that is, the peak point of ion density profile, i.e., electron density exists in front of the plug potential peak point.This means that the electrostatic potential around plug region does not obey the traditional Boltzmann law.

Therefore, the electron distribution function is found to be non-Maxwellian. The actual electron distribution function should be determined including the effects of ECRH and other loss processes. But this is difficult in general so that we include the effect of non-Maxwellian electrons by assuming the electron distribution function in eq. (2).

Figure 3 shows the plug potential in the steady state for the case of $T_{e\perp}/T_i = 30$ and $T_{e\parallel}/T_i = 1$. Here the used parameters are that the electrostatic potential is $e\varphi_i/T_i = 0$ at the inner mirror throat, and $e\varphi_b/T_i = -2$ at thermal barrier.

Figure 3(a) displays the steady state electrostatic potential and ion density axial profiles. It is seen that the peak point of ion density locates in front of the electrostatic potential maximum. The plug (where the electrostatic potential is maximum) exists in the midway from thermal barrier region to the outer mirror throat. The height of the plug potential is $e\varphi_p/T_i = 1.8$ in Fig. 3(a). The difference between the ion density axial profile and electrostatic potential profile results from the non-Maxwellian electron distribution function. A large majority of ions, the mean velocity of which is about thermal velocity, reflects at the region where the electrostatic potential is slightly larger than that at the inner mirror throat in Fig. 3(a).

The remarkable feature in Fig. 3(a) is that the continuous electrostatic potential is realized especially around the plug region. The charge neutrality condition is assumed in the simulation so that the discontinuous electrostatic potential can appear where the charge neutrality condition breaks such as sheath potential formation. As mentioned in ref. [3] the discontinuous electrostatic potential profile will appear around the plug if no ions come from the outer mirror throat. It is enough to make the electrostatic potential continuous

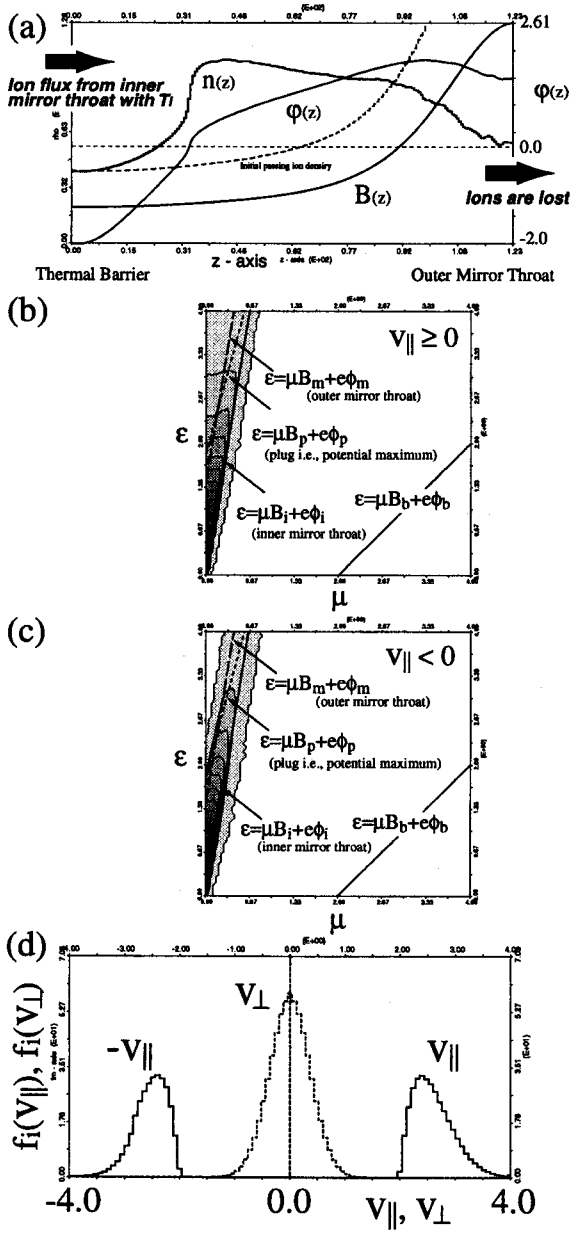

Fig. 3 The steady state axial profiles. (a) is the ion density and electrostatic potential axial profiles, where dashed line is the initial ion density profile in $\varphi(z) = 0$. (b) and (c) are ion velocity space represented by ε and μ, where broken line is $\varepsilon = \mu B_m + e\varphi_m$, and dashed line is $\varepsilon = \mu B_p + e\varphi_p$, respectively. (d) is the ion distribution function observed in the region $0 \le z \le 1$ cm.

even if the population of those ions from outer mirror throat is very few.

The Figs. 3(b) and 3(c) plot the ion velocity space represented by ε and μ, where $v_{\parallel} \geq 0$ is in Fig. 3(b) and $v_{\parallel} < 0$ is in Fig. 3(c). The ions are input at the inner mirror throat i.e., Maxwellian ions are seen in the region $\varepsilon - \mu B_i - e\varphi_i \geq 0$ in Fig. 3(b). On the other hand the ions in the region $\varepsilon - \mu B_p - e\varphi_p \geq 0$ and $\varepsilon - \mu B_m - e\varphi_m \geq 0$ are lost at the outer mirror throat. It is seen that the Maxwellian ions exist in the region of loss conein Fig. 3(b), while very few ions are found there in Fig. 3(c).

The ion distribution function around the thermal barrier region ($0 \leq z \leq 1$ cm) is plotted in Fig. 3(d). There is no ions with small velocity of $v_{\parallel}$. It is found that the perpendicular ion temperature around the thermal barrier region is less than unity which is the temperature given at the inner mirror throat. The reason why the perpendicular temperature is small is that the ions are accelerated by magnetic field from the inner mirror throat to the thermal barrier and the perpendicular kinetic energy is changed to the parallel kinetic energy.

Figure 4 displays the ion density and electrostatic potential axial profiles in the steady state in the case that the magnetically trapped high energy electrons are exist, where the modified Boltzmann law is given as

$$\varphi(z) = \frac{T_{e\parallel}}{e} \ln \left\{ \left[\frac{T_{e\perp}}{T_{e\parallel}} + \left(1 - \frac{T_{e\perp}}{T_{e\parallel}} \right) \frac{B_b}{B(z)} \right] \frac{n(z) - n_h(z)}{n_b - n_h(z_b)} \right\}. \tag{5}$$

Here

$$n_h(z) = 0.8 \times n_b \frac{B(z) - B_m}{B_b - B_m}. \tag{6}$$

In the case including the magnetically trapped electron population, high plug potential $e\varphi_p/T_i = 2.4$ is realized in Fig. 4.

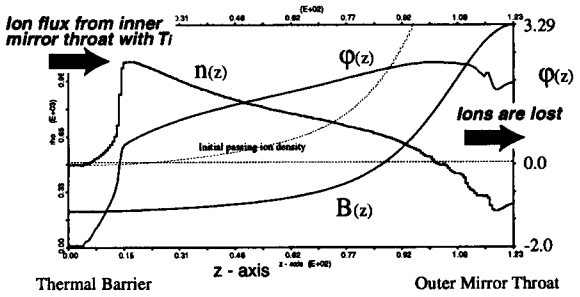

Fig. 4 Ion density and electrostatic potential axial profiles. Here dashed line is initial ion density profile in $\varphi(z) = 0$.

4. Summary

We have shown by the Monte-Carlo simulation that the plug potential can be formed only with the ions flowing from the inner mirror throat and non-Maxwellian electron population. The essential point for the large plug potential formation is that the electron distribution function is non-Maxwellian. Otherwise, the density maximum point coincides with the plug point, which is inconsistent with the fact that the majority of ions reflects in front of the plug point. The effects of ECRH is included in the non-Maxwellian electrons.

The previous works for the plug potential formation [1-4] made use of the simplified ion distribution function so that the artificial dissipation such as the ionization effect was required in order to obtain the continuous electrostatic potential profile across the plug region. In this work, however, each ion motion is followed numerically in the magnetic mirror cell and the coulomb scattering is included as the effects of dissipation by Monte-Carlo simulation but without any other dissipation such as ionization effects, so that the plug potential formation have been demonstrated in the more realistic condition.

References

[1] I. Katanuma, Y. Kiwamoto, Y. Tatematsu, K. Ishii, T. Saito, K. Yatsu and T. Tamano, Phys. Plasmas **3**, 2218 (1996).

[2] T. Saito, I. Katanuma, T. Aota, L.G. Bruskin, T. Cho, *et al.*, Fusion Energy **2**, 105 (1997).

[3] I. Katanuma, Y. Kiwamoto, Y. Tatematsu, K. Ishii, T. Saito, K. Yatsu and T. Tamano, Phys. Plasmas **4**, 2532 (1997).

[4] I. Katanuma, Y. Kiwamoto, Y. Tatematsu, K. Ishii, T. Saito, T. Tamano and K. Yatsu, Phys. Plasmas **5**, 1560 (1998).

[5] I. Katanuma, Y. Kiwamoto, M. Ichimura, T. Saito and S. Miyoshi, Phys. Fluids B **2**, 994 (1990).

[6] R. Minai, I. Katanuma and T. Tamano, J. Phys. Soc. Jpn. **66**, 2051 (1997).

[7] R. Minai, I. Katanuma, T. Tamano and K. Yatsu, J. Phys. Soc. Jpn. **67**, 876 (1998).